Regenerative Therapy 25 (2024) 162–173

Contents lists available at ScienceDirect

Regenerative Therapy

journal homepage: http://www.elsevier.com/locate/reth

Original Article

Bi-functional KIT-PR1P peptides combine with VEGF to protect ischemic kidney in rats by targeting to Kim-1

Runxue Zhou [a, 1], Hang Liu [b, 1], Xianglin Hou [c, 1], Qi Liu [a, d], Shuwei Sun [a], Xiaoge Li [e], Wenxuan Cao [a], Weihong Nie [a], Chunying Shi [a, *], Wei Chen [f, **]

[a] Department of Human Anatomy, Histology and Embryology, School of Basic Medicine, Qingdao University, Qingdao, 266071, China
[b] Department of Nephropathy, The Affiliated Hospital of Qingdao University, Qingdao, 266700, China
[c] State Key Laboratory of Molecular Developmental Biology, Institute of Genetics Cand Developmental Biology, Chinese Academy of Sciences, Beijing, 100190, China
[d] Department of Neurology, The Affiliated Hospital of Qingdao University, 16 Jiangsu Road, Qingdao, Shandong, 266000, China
[e] Department of Biochemistry and Molecular Biology, School of Basic Medicine, Qingdao University, Qingdao, 266071, China
[f] Department of Urology, Xinqiao Hospital, Army Medical University, Chongqing, 400038, China

ARTICLE INFO

Article history:
Received 21 October 2023
Received in revised form
13 December 2023
Accepted 21 December 2023

Keywords:
Vascular endothelial growth factor
Acute kidney injury
Targeted delivery
Kidney injury molecular-1
Tissue regeneration

ABSTRACT

Introduction: Acute kidney injury (AKI) was a disease with a high mortality mainly caused by renal ischemia/reperfusion injury (I/R). Although the current non-targeted administration of vascular endothelial growth factor (VEGF) for AKI had been revealed to facilitate the recovery of renal I/R, how to targeted deliver VEGF and to retain it efficiently in the ischemic kidney was critical for its clinical application.

Methods: In present study, bi-functional KIT-PR1P peptides were constructed which bond VEGF through PR1P domain, and targeted ischemic kidney through KIT domain to interact with biomarker of AKI-kidney injury molecule-1 (Kim-1). Then the targeted and therapeutic effects of KIT-PR1P/VEGF in AKI was explored *in vitro* and *in vivo*.

Results: The results showed KIT-PR1P exhibited better angiogenic capacity and targeting ability to hypoxia HK-2 cells with up-regulated Kim-1 *in vitro*. When KIT-PR1P/VEGF was used for the treatment of renal I/R through intravenous administration *in vivo*, KIT-PR1P could guide VEGF and retain its effective concentration in ischemic kidney. In addition, KIT-PR1P/VEGF promoted angiogenesis, alleviated renal tubular injury and fibrosis, and finally promoted functional recovery of renal I/R.

Conclusion: These results indicated that the bi-functional KIT-PR1P peptides combined with VEGF would be a promising strategy for the treatment of AKI by targeting to Kim-1.

1. Introduction

Acute renal injury (AKI) was a common renal disease. It was usually characterized by rapid loss of renal function and decreased glomerular filtration rate, which might develop into chronic kidney disease (CKD) and end-stage renal disease (ESRD) [1]. Renal ischemia reperfusion (I/R) as the main factor of AKI, caused the death of renal tubular epithelial cells and vascular endothelial cells, but also impacted the morphology and function of renal tubule, eventually led to renal interstitial fibrosis. Therefore, increasing renal blood flow and protecting the renal cells from damage would attenuate I/R renal injury [2,3].

Vascular endothelial growth factor (VEGF) was a highly specific vascular growth factor. After ischemic injury of kidney, VEGF could induce angiogenesis by promoting endothelial cells proliferation and also protect renal cells from I/R injury. Thus, it was reported to improve the renal function and inhibit tissue fibrosis of further development of AKI [4]. At present, the administration of VEGF after AKI often utilized intraperitoneal, intravenous or subcutaneous intrarenal injection. These routes were non-targeted and rapid diffusion might cause undesirable side effects. As a result, it was urgent to explore a safe and efficient delivery strategy of VEGF for the treatment of AKI.

* Corresponding author.
** Corresponding author.
E-mail addresses: schy1116@163.com (C. Shi), doctorcw@126.com (W. Chen).
Peer review under responsibility of the Japanese Society for Regenerative Medicine.
[1] means co-first author.

https://doi.org/10.1016/j.reth.2023.12.014

When tissues or organs were injured, series of specific molecules upregulated in the tissue microenvironment, which were potential targets for the spatiotemporal delivery of growth factors [5,6]. As one of the important signs of early acute renal injury, kidney injury molecule-1 (Kim-1, also known as hepatitis A virus cell receptor-1 or T cell Ig mucin-1) significantly increased by 3–100 times after acute renal ischemia or renal tissue injury, but decreased rapidly in the stage of renal fibrosis and remodelling [7,8]. Recent studies had proved that Kim-1 was a reliable biomarker of acute renal injury, but also an important target for the treatment of renal tubular injury [9,10]. In 2019, Enamul Haque et al. screened a specific short peptide KIT through phage display [11]. This short peptide could specifically bind with the cells expressing Kim-1, which had potential guiding ability of VEGF for acute renal injury. In our previous study, we had designed and prepared targeting peptide modified recombinant VEGF proteins such as collagen binding CBD-VEGF, ischemic myocardium targeting IMT-VEGF. However, the purification of modified VEGF was difficult, because refolding of genetic engineering VEGF protein from inclusion bodies was needed. Thus, how to connect KIT peptide with VEGF conveniently would be beneficial for the targeting repair of VEGF in AKI.

Currently, a specific peptide PR1P deriving from the interacting protein of VEGF-Prominin-115, was reported to specifically bind to VEGF [12]. Unlike physical encapsulation, electrostatic interaction or covalent coupling, PR1P peptide bond to VEGF with high specificity in natural state and enhanced VEGF dimer formation to improve its biological activity [13]. In this paper, a bi-functional KIT-PR1P was constructed that could combine and guide VEGF to ischemic kidney by targeting to Kim-1. We explored the targeted and therapeutic effect of KIT-PR1P/VEGF in acute renal ischemia injury *in vitro* and *in vivo*.

2. Materials and methods

2.1. Synthesis of KIT-PR1P and PR1P peptides and preparation of VEGF

The PR1P peptides (DRVQRQTTTVVA) and KIT-PR1P peptides (DRVQRQTTTVVAGSAGSAAGSGGCNWMINKEC) were synthesized by the Sagon Inc. (Shanghai, China) with the purity greater than or equal to 98 %. And the FITC-modified PR1P or KIT-PR1P peptides were also chemically synthesized and modified by the Sagon Inc. (Shanghai, China) with the purity greater than or equal to 98 %. Recombinant VEGF was prepared by Ni-column as described previously [14]. For the construction of the KIT-PR1P/VEGF delivery system, the KIT-PR1P was mixed with VEGF at 4 °C at 2:1 molecular weight for 3 h.

2.2. Determination of targeted binding ability of KIT-PR1P on hypoxia HK-2 cells and biological activity assay

The 96-well plates and assembled matrix gel (Corning, 356234) were pre-cooled overnight. 50 μl/well of matrix gel was added to the 96-well plates and placed in a cell incubator for 45–60 min until cured. HUVECs (9×10^4 cells/well) were then inoculated onto Matrigel layers and divided into 3 groups: control (DMEM, 2 % FBS), VEGF (DMEM, 2 % FBS, 50 ng/ml VEGF), KIT-PR1P/VEGF (DMEM, 2 % FBS, 50 ng/ml KIT-PR1P/VEGF). 3 wells per group, 5 non-overlapping fields of view were selected for detection in each well. Image J software's tool-Angiogenesis Analyzer was used to count tubular structures and network branches [15], and then angiogenic network formation was quantified by GraphPad Prism 8.

Immunofluorescence co-staining experiments with Kim-1 and VEGF in HK-2 cells were performed as follows: HK-2 cells were inoculated into 48-well plates at a density of 1.4×10^4/L as described above until the cell density was 70%–80 %, the original medium was discarded, and HK-2 complete medium containing 2 % serum separately mixed with 50 ng/ml KIT-PR1P/VEGF, PR1P/VEGF and an equal amount of PBS. cells were co-cultured under hypoxic conditions (5%CO_2, 95%N_2) for 12 h and then reoxygenated for 3 h. Subsequently, the cells were fixed using 4 % histiocyte fixative for 20 min, and the plate of wells in which the cells had been fixed was washed with a bubble of PBS three times for 10 s each, and after aspirating the liquid, the cells were permeabilised with 0.3 % Triton (200ul per well). This process was carried out on a shaker (100 rpm, 20min), after the permeabilisation was completed, the plate was continued to be washed 3 times with PBS for 5min each time. Afterwards, 3 % BSA solution was prepared in PBS, and 200ul of 3 % BSA solution was added to each well to seal the cells in the plate for 30 min, after which the liquid was discarded, and 50ul of configured VEGFA Monoclonal antibody (1:400, Mouse/IgG2b, Proteintech, China) and Kim-1 antibody (1:400, Rabbit/IgG2b, Novus, America)were added to each well to incubate overnight at 4 °C for 16 h. The primary antibody in the wells was discarded and washed three times with PBS for 5 min each time, followed by 50ul of Goat Anti-Rabbit IgG H&L (Alexa Fluor® 594, 1:400, Abcam) and Goat Anti-Mouse IgG H&L (Alexa Fluor® 488, 1:400, Abcam) which were incubated at room temperature and protected from light for 1 h. The wells were washed three times with PBS for 5 min each time, and DAPI Staining Solution (C1005, Beyotime, Shanghai, China) was used to stain the nuclei of the cells, 100ul of DAPI Staining Solution was added to each well, and the cells were incubated at room temperature and protected from light for 5 min, DAPI Staining Solution was aspirated, and washed with PBS 3 times, each time for 5 min 200ul of PBS was retained in each well. The distribution of VEGF (green fluorescence) and Kim-1 (red fluorescence) in each group (12wells/group) was observed by inverted fluorescence microscope, 3 non-overlapping fields of view for each well were selected to detect the regional fluorescence intensity. The regional fluorescence intensity data was analyzed as Integrated Density by Image J and GraphPad Prism 8, and the fluorescence overlap of VEGF and Kim-1 was observed. The Fluorescence co-localization analysis was made by Image J's Plot Profile tool Based on Pearson's co-location analysis.

2.3. Construction of renal I/R injury model in rats

All of the animal experiments were performed according to local Guidelines on the ethical use of animals and the National Institutes of Health'Guide for the Care and Use of Laboratory Animals' (NIH publication23–80,revised2011), and all protocols were approved by Animal Care and Use Committee of Qingdao University. Female Sprague Dawley rats (200–240 g, 8–10 weeks old) were purchased from Jinan Pengyue Experimental Animal Breeding Co. Ltd., and the rats were housed in a specific pathogen-free facility with the temperature of 25 °C and cycle with 40–60 % relative humidity in 12 h/12 h light/dark. The rats were anesthetized with 8 % Chloral hydrate (50 mg/kg) by intraperitoneal injection. After the right nephrectomy, the left renal artery was clamped for 45 min and reperfusion for 1 h. A series of experiments were performed to test the targeting ability and the protective effect of KIT-PR1P/VEGF or native VEGF.

2.4. Quantitative ELISA analysis of KIT-PR1P/VEGF in vivo

After kidney ischemia injury and a 1 h reperfusion, KIT-PR1P/VEGF (0.05 mg/kg), KIT-PR1P (0.05 mg/kg), PR1P/VEGF (0.05 mg/kg), native VEGF (0.05 mg/kg) and Equivalent amount of PBS were injected into the renal I/R rat through tail vein. At 6 and 24 h post-

administration, the ischemic kidney and serum were harvested. And then, extracted proteins and serum were analyzed using a human VEGF ELISA kit (Boster, Wuhan, China) according to the protocol.

2.5. Fluorescent imaging of KIT-PR1P and PR1P in the ischemic kidney in vivo

KIT-PR1P or PR1P were fluorescently labelled by FITC. After hypoxia injury and 1 h reperfusion, the I/R rat model was injected with 100 μl fluorescent-labelled KIT-PR1P or PR1P proteins through the tail vein. At 6 and 24 h after administration, the animals were sacrificed and kidneys were immediately harvested to prepare frozen sections. Finally, the distribution of FITC-labelled peptides was observed by fluorescence microscope. 3 non-overlapping fields of view for each section were selected to detect the mean fluorescence intensity, 5 section in a group. The mean fluorescence intensity of FITC (green fluorescence) was counted by Image J, the statistics were analysed by GraphPad Prism 8.

2.6. Assessment of renal function in rats with renal I/R injury

The animals were randomly divided into four groups: normal group (sham), I/R group including KIT-PR1P/VEGF group, native VEGF group and PBS group (control). Rats were anesthetized with 8 % Chloral hydrate (50 mg/kg) by intraperitoneal injection. In the I/R group, after the right nephrectomy, the left renal artery was clamped for 45 min and reperfusion for 1 h, and then KIT-PR1P/VEGF (0.05 mg/kg), native VEGF (0.05 mg/kg) or PBS were injected through caudal vein. A series of experiments were performed to test the targeting ability and the protective effect of KIT-PR1P/VEGF or native VEGF. Rats' serum was taken at 24, 72 h and 2w after administration for assessment renal function. Renal function was assessed based on serum creatinine (SCRA). Creatinine (Cr) Assay Kit (Nanjing Jiancheng, China) was used for the assay of Scr.

2.7. HE&MASSON

The isolated kidney tissues were fixed with 4 % paraformaldehyde solution for 12 h. The soaked samples were embedded in paraffin and sliced into 4-μm slices. Haematoxylin-eosin staining (H&E) was performed to detect the damage of renal tubules and glomerulus. A 5-point scoring system was developed to determine tubular injury by assessing tubular epithelial necrosis, tubular dilatation, loss of brush border and cast formation, as shown below: 0-point: normal or none; 1-point: damage of tubules $\leq$10 %; 2-point: damage of tubules 11–25 %; 3-point: damage of tubules 26–45 %; 4-point: damage of tubules 46–75 %; 5-point: damage of tubules $\geq$76 %. For each H&E staining sample, at last 10 contiguous areas of the cortical medulla junction and the external medulla were examined in each section. Masson's trichrome staining was performed to detect renal fibrosis. Five blue areas of non-overlapping visual field were randomly selected from each kidney section. The results were analysed using Image Pro-Plus v. 6.0 software (Bethesda, MD, USA).

2.8. TUNEL

TUNEL (TdT Mediated dUTP Nick End Labelling) apoptosis Detection Kit (Alexa Fluor 488) (Yeasen, Shanghai, China) was used to detect nuclear DNA breaks during late apoptosis. In apoptotic nucleus, TUNEL-positive nucleus (green) was labelled by fluorescein 488. 5 non-overlapping fields of view were selected for each section to observe the number of positive cells, and the counts of positive cells (green fluorescent labelled cells) and total cells (DAPI) in the corresponding field of view were analyzed by Image J, TUNEL apoptotic cell rate = number of positive cells/total cells × 100 %, and the data were analyzed by GraphPad Prism 8.

2.9. Immunofluorescence staining

At 6 h and 24 h after drug administration, the ischemic kidneys were immediately fixed and paraffin sections were prepared. Immunofluorescence staining was performed on paraffin sections as the same as Immunohistochemical staining slices. The primary antibodies included VEGFA Monoclonal antibody (1:400, Mouse/IgG2b, Proteintech, China) and Kim-1 antibody (1:400, Rabbit/IgG2b, Novus, America). Both primary antibodies were incubated with slices overnight at 4 °C. The slices were exposed to Goat Anti-Rabbit IgG H&L (Alexa Fluor® 594, 1:400, Abcam) and Goat Anti-Mouse IgG H&L (Alexa Fluor® 488, 1:400, Abcam) at room temperature for 1 h. After sealing by DAPI, the sections were observed using fluorescence microscopes. For each paraffin section, 5 non-overlapping fields of view were selected to detect the regional fluorescence of green fluorescence and red fluorescence, and the regional fluorescence intensity was analyzed by Image J as Integrated Density and GraphPad Prism 8, and the fluorescence overlap of VEGF and Kim-1 was observed. The Fluorescence co-localization analysis was made by Image J's Plot Profile tool Based on Pearson's co-location analysis.

At 24 h, 72 h and 2w after drug administration, the ischemic kidneys were immediately fixed and paraffin sections were prepared. Immunofluorescence staining was performed on paraffin sections as the same as Immunohistochemical staining slices. The primary antibodies included rabbit anti-CD31 (1: 200; Zen Bioscience, Chengdu, China) and rabbit anti-p-VEGFR (1: 500; Abclonal, America). Both primary antibodies were respectively incubated with slices overnight at 4 °C. The slices were exposed to Goat Anti-Rabbit IgG H&L (Alexa Fluor® 488, 1:500; Abcam, America) at room temperature for 1 h. After sealing by DAPI, the sections were observed using fluorescence microscopes. For each paraffin section, 5 non-overlapping fields of view were selected to detect the mean fluorescence intensity of green fluorescence, and the mean fluorescence intensity data were analyzed by Image J and GraphPad Prism 8.

Immunofluorescence staining for cleaved Caspase-3: Primary antibody was rabbit anti-cleaved Caspase-3 (1:400; Proteintech, China). The primary antibody was incubated with the sections at 4 °C overnight. Sections were reacted with goat rabbit polyclonal secondary antibody (Alexa Fluor® 594, 1:500; Abcam, USA) for 1 h at room temperature. After sealing by DAPI, the sections were observed using fluorescence microscopes. For each paraffin section, 5 non-overlapping fields of view were selected to detect the Integrated Density of red fluorescence, and the Integrated Density data were analyzed using Image J and GraphPad Prism 8.

2.10. Western blotting

Proteins supernatant was extracted from kidney and analyzed by Western blotting. Equal amounts of proteins were separated by SDS-PAGE and transferred to PVDF membranes. The membrane was then blocked with skimmed milk for 1 h, incubated with primary antibody overnight at 4 °C. After cleaning with TBST, the membranes were incubated with Goat Anti-rabbit HRP antibody (1:5000; Bioss, Beijing, China) at room temperature for 1 h and the signals were detected with the Omin-ECL ultra-sensitive chemiluminescence detection kit (EpiZyme, Shanghai, China), and their intensities were measured with Image J 6.0 software and analyzed by GraphPad Prism 8. Primary antibodies used in this study included anti-VEGF (1 : 1000 , ZEN-BIOSCIENCE, China), anti-p-

VEGFR (1:1000, Abclonal), anti-AKT (1:1000; ZEN-BIOSCIENCE, Chengdu, China), anti-p-AKT (1:1000; ZEN-BIOSCIENCE, Chengdu, China), anti-ERK1/2 (1:1000; ZEN-BIOSCIENCE, Chengdu, China), anti-p-ERK1/2 (1:1000; Boster, Wuhan, China; 1:1000,Abclonal) and anti-GAPDH (1:1000; Proteintech), GAPDH served as an internal control.

2.11. Statistical analysis

All data was expressed as the mean ± standard deviation (SD). GraphPad Prism v. 8.00 was used to analyse the statistics and comparisons between multiple groups were performed using one-way ANOVA. Student's t-test was performed with SPSS. One-way ANOVA was used for renal function, H&E, Masson, CD31, TUNEL, cleaved Caspase-3, Vimentin and p-VEGFR. Student's t-test was used for the bioactivity of KIT-PR1P/VEGF and native VEGF. The level of $P < 0.05$ represented statistical significance. Data were expressed as mean ± SD.

3. Results

3.1. The bioactivity and targeting ability of KIT-PR1P in vitro

It had been shown PR1P could bind with VEGF and enhance the bioactivity of VEGF. Then we firstly detected the bioactivity of KIT-PR1P/VEGF by the *in vitro* tube-formation assay of HUVECs. As shown in Fig. 1 (A-D), the number of tube-like structures in KIT-PR1P/VEGF group was significantly higher than that in VEGF group and control group. These results showed that KIT-PR1P/VEGF had a stronger ability to promote angiogenesis *in vitro*. In addition, it was reported Kim-1 upregulated significantly after hypoxia-treated HK-2 cells *in intro* [16]. The binding ability of KIT-PR1P and PR1P with hypoxic HK-2 cells was detected. Firstly, the KIT-PR1P and PR1P were labelled with fluorescent-FITC. As shown in Supplementary Fig. 1 (A-C), the mean fluorescence intensity of KIT-PR1P-FITC was significantly higher than that of PR1P-FITC. Furthermore, KIT-PR1P aimed to bind and guide VEGF to hypoxic HK-2 cells with high expressed Kim-1, whether KIT-PR1P/VEGF could target to Kim-1 on hypoxic HK-2 cells was assessed. And the immunofluorescence colocalization staining of VEGF and Kim-1 was performed after KIT-PR1P/VEGF incubated with hypoxic HK-2 cells. The results showed the fluorescence intensity of VEGF in KIT-PR1P/VEGF group was significant upregulated compared with other two groups, while the expression of Kim-1 was upregulated in all the three groups without statistical difference (Fig. 1E and F). And most of VEGF in KIT-PR1P/VEGF group was colocalized with Kim-1 but there was less colocalization of VEGF and Kim-1 observed in VEGF group and PBS group with significant difference (Fig. 1G–I). These results suggested that KIT-PR1P/VEGF had better targeted ability to hypoxic HK-2 cells with high expression of Kim-1.

3.2. KIT-PR1P/VEGF targeted and retained in the ischemic kidney in vivo after intravenous injection

After confirming the binding ability of KIT-PR1P/VEGF on hypoxia HK-2 *in vitro*, we explored the targeting ability of KIT-PR1P/VEGF *in vivo* further. Firstly, KIT-PR1P-FITC and PR1P-FITC were injected into rats through the tail vein. At 6 h and 24 h after injection, the average fluorescence intensity of renal tissue was observed under fluorescence microscope. The results showed the average fluorescence intensity of KIT-PR1P-FITC group was significantly higher than that of PR1P-FITC group at both 6 h and 24 h after injection (Supplementary Fig. 2A–D). Then whether KIT-PR1P could guide VEGF to the ischemic kidney with high expressed Kim-1 was investigated, and the immunofluorescence colocalization staining of VEGF and Kim-1 was performed in ischemic kidney at 6 h and 24 h after injection. The results showed at 6 h after injection, more VEGF accumulated in KIT-PR1P/VEGF group (24.60 ± 12.33, 42.82 ± 25.27), which had significantly stronger mean fluorescence intensity than PR1P/VEGF group (10.79 ± 7.95, 7.13 ± 6.16), VEGF group (4.47 ± 1.91,8.94 ± 5.11) and PBS group (3.17 ± 3.54, 3.61 ± 3.33) (Fig. 2A, C). Moreover, better co-localization of VEGF and injured marker-Kim-1 was observed compared with the other three groups as shown in Fig. 2E. In addition, similar results were observed at 24 h after injection (Fig. 2B, D, F). These results demonstrated the KIT-PR1P/VEGF had specific homing potential to the ischemic kidney targeting Kim-1 *in vivo*. Finally, the content of VEGF in ischemic kidneys was quantified (Fig. 2G). The results showed that the VEGF content in ischemic kidney was significantly higher in the KIT-PR1P/VEGF group (0.616 ± 0.077 μg/g) than that of PR1P/VEGF group (0.406 ± 0.033 μg/g), VEGF group (0.449 ± 0.027 μg/g), KIT-PR1P group (0.429 ± 0.057 μg/g) and PBS group (0.266 ± 0.019 μg/g) at 6 h after injection, and there was also significant difference between PR1P/VEGF group, VEGF group, KIT-PR1P group and PBS group. And at 24 h after injection, the content of VEGF in ischemic kidney of KIT-PR1P/VEGF group (0.378 ± 0.041 μg/g) was also statistically higher than that of PR1P/VEGF group (0.254 ± 0.041 μg/g), VEGF group (0.185 ± 0.025 μg/g), KIT-PR1P group (0.278 ± 0.031 μg/g) and PBS group (0.162 ± 0.060 μg/g). There was no difference between PR1P/VEGF group, VEGF group and PBS group but KIT-PR1P group had statistical difference with PBS group. Then the content of VEGF in serum was also detected (Fig. 2H). Although the KIT-PR1P/VEGF group had slightly lower levels of VEGF in serum which had significant difference with PR1P/VEGF group but there was no difference between KIT-PR1P/VEGF group and VEGF group, KIT-PR1P group, PBS group at 6 h after injection; at 24 h after injection, there was no statistical difference was observed among all these group. In addition, the expression of VEGF in ischemic kidney were further confirmed by Western blot which was consistent with the result of Elisa assays (Fig. 2I). The above results indicated that KIT-PR1P/VEGF could target to injured renal tubular cells with high expressed Kim-1 that specifically retained VEGF in ischemic kidney by intravenous injection.

3.3. KIT-PR1P/VEGF improved the recovery of renal function after acute renal I/R injury

We verified whether KIT-PR1P/VEGF was effective in protecting the kidney following I/R injury. Renal function was assessed by the gold standard — serum creatinine (Scr) level (Fig. 3). The level of Scr in the KIT-PR1P/VEGF group (134.76 ± 60.08umol/L) was significantly lower than that in the VEGF (192.62 ± 75.01umol/L) and PBS (350.03 ± 106.33umol/L) groups at 24 h after intravenous injection ($P < 0.05$). Over time, there was a certain degree of recovery in all groups, but the level of Scr in the KIT-PR1P/VEGF group was still significantly less than that in the other two groups ($P < 0.05$). These results revealed that due to targeted delivery, KIT-PR1P/VEGF could effectively improve the recovery of renal function compared to that in the VEGF and PBS groups after acute I/R injury.

3.4. KIT-PR1P/VEGF effectively protected renal tissue from ischemic injury and reduced morphological damage to the kidney

Pathological examinations were evaluated at 24 h, 72 h and 2w after injection. Histopathological staining (H&E staining) was used to assess renal morphological damage. As shown in Fig. 4 A-F, there was no apparent renal damage in the normal group, whereas PBS-injected rats showed severe renal damage, cast formation,

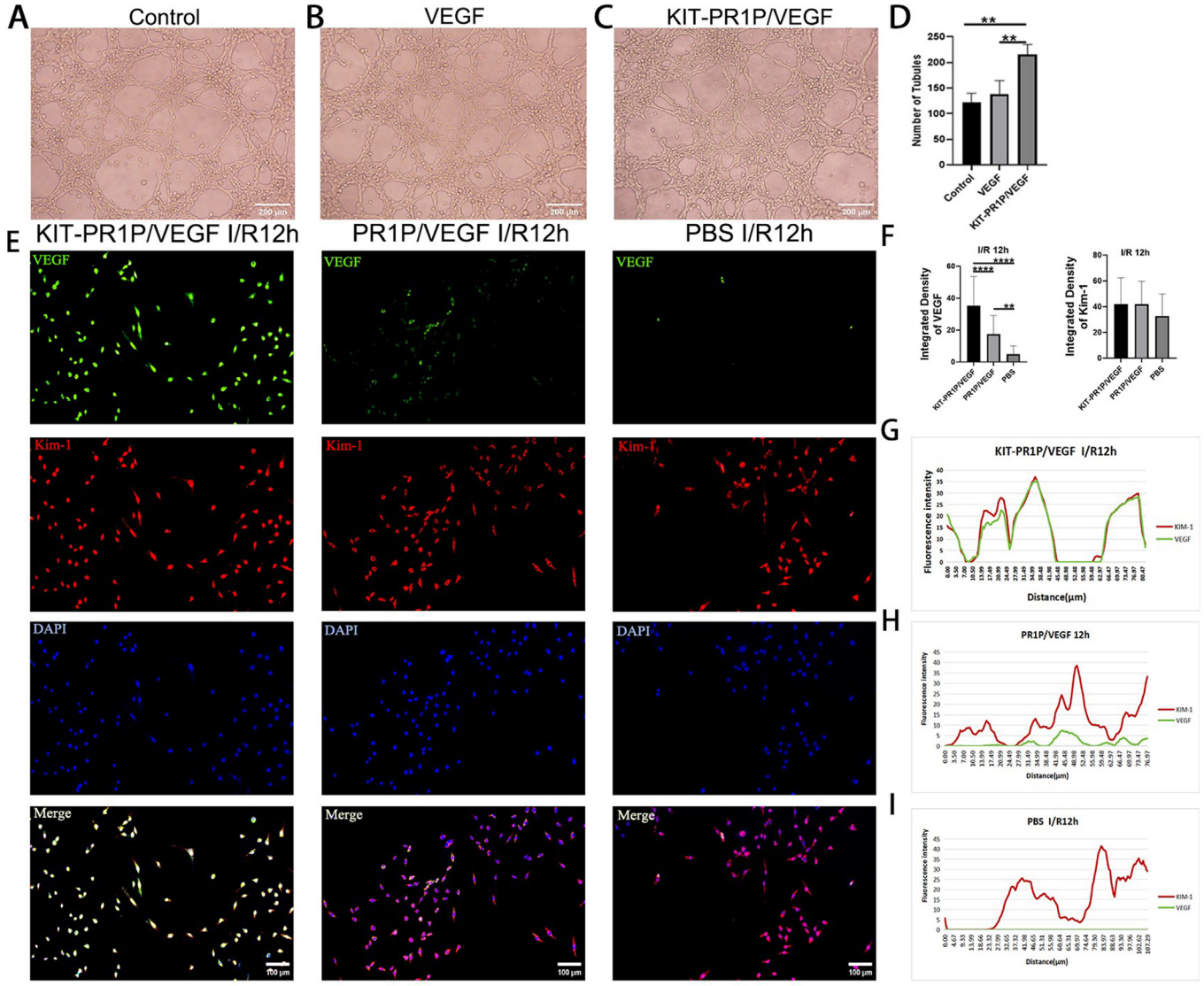

Fig. 1. The bioactivity and targeting ability of KIT-PR1P. (A–D) The angiogenic ability of KIT-PR1P/VEGF and natural VEGF. N = 3. The Scale Bar = 200 μm **P < 0.01. (E) The targeting ability of KIT-PR1P/VEGF and PR1P/VEGF in hypoxic HK-2 cells was verified by immunofluorescence of the renal tubular injury marker Kim-1 and VEGF co-staining assay. VEGF (green), the renal tubular injury marker Kim-1 (red), DAPI (blue). Yellow staining indicates co-localization. The Scale Bar = 100 μm. (F) Fluorescence Integrated density of VEGF (35.34 ± 18.22, 17.48 ± 11.65, 4.89 ± 5.18) and Kim-1 (47.15 ± 23.47, 30.54 ± 15.99, 32.28 ± 17.85) in the KIT-PR1P/VEGF group, PR1P/VEGF group and PBS group. ****P < 0.0001, **P < 0.01.All data are expressed as mean ± SD. (G) Fluorescence co-localisation analysis of Kim-1and VEGF in the KIT-PR1P/VEGF group. (H) Fluorescence co-localisation analysis of Kim-1 and VEGF in the PR1P/VEGF group. (I) Fluorescence co-localisation analysis of Kim-1 and VEGF in the PBS group.

abundant tubular epithelial necrosis and increased tubular dilatation and congestion. In addition, the tubules exhibited massive proteinuria, and the glomerulus was heavily congested, whereas treatment with KIT-PR1P/VEGF and VEGF decreased tubule damage, congestion and cast formation. Rats treated with KIT-PR1P/VEGF had mild damage to renal tubules; most tubules had intact shapes and reduced congestion among the three treatment groups. The renal tubular injury scores also showed that treatment with KIT-PR1P/VEGF (1.60 ± 0.55, 2.20 ± 0.45, 2.20 ± 0.45) markedly reduced the renal damage scores compared to VEGF (2.40 ± 0.55, 2.60 ± 0.55 , 3.17 ± 0.41) and PBS (2.80 ± 0.45, 3.20 ± 0.45, 3.50 ± 0.55) at 24 h, 72 h and 2w after intravenous injection. These results demonstrated that KIT-PR1P/VEGF could effectively protect the kidney against renal I/R injury.

In addition, it was reported that the progressive loss of kidney function until the terminal stage was a typical characteristic of CKD. The most significant manifestation was morphological changes, including tubular fibrosis and glomerular sclerosis. Both conditions led to progressive destruction and irreversible damage to the kidneys [17,18]. Thus, Masson's trichrome staining was used to assess renal fibrosis at 72 h and 2w after injection (Fig. 4J and K). No apparent renal fibrosis was observed in the normal (7.29 ± 4.21 %) group. Treatment with KIT-PR1P/VEGF (19.93 ± 4.53 %, 20.92 ± 9.06 %) significantly attenuated renal fibrosis (blue staining), and the fibrotic area was significantly less than that in the VEGF-treated (27.46 ± 4.68 %, 37.06 ± 5.81 %) and PBS-treated (35.04 ± 7.07 %, 40.68 ± 8.82 %) groups. Therefore, KIT-PR1P/VEGF played an important role in decreasing renal fibrosis after renal I/R injury.

3.5. KIT-PR1P/VEGF repaired the kidney after renal I/R injury by promoting angiogenesis

VEGF was the most potent angiogenic growth factor, so we detected the angiogenesis in ischemic kidney [19–21]. CD31 immunofluorescence staining results showed significantly higher

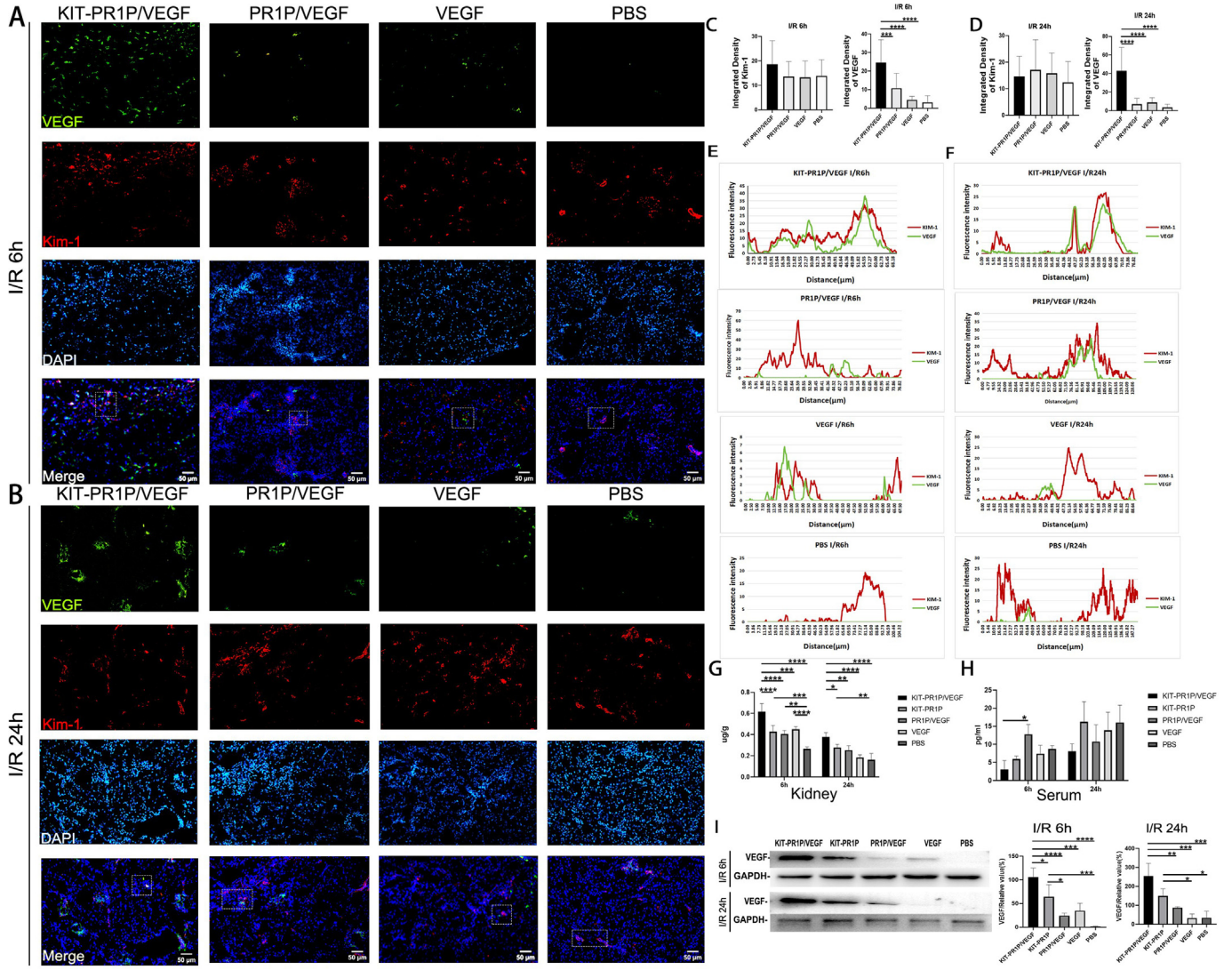

Fig. 2. The targeting ability of KIT-PR1P/VEGF *in vivo*. (A–B) Immunofluorescence co-staining assay. for VEGF (green) and the renal tubular injury marker Kim-1 (red) at 6 h and 24 h post-administration. DAPI (blue). The Scale Bar = 50 μm. (C) Fluorescence Integrated density of VEGF (24.60 ± 12.33, 10.79 ± 7.95, 4.47 ± 1.91, 3.17 ± 3.54) and Kim-1 (18.63 ± 9.67, 13.61 ± 6.10,13.23 ± 6.75, 13.85 ± 6.62) in the KIT-PR1P/VEGF group, PR1P/VEGF group, VEGF group and PBS group at I/R 6 h. ****P < 0.0001, ***P < 0.001.All data are expressed as mean ± SD. (D) Fluorescence Integrated density of VEGF (42.82 ± 25.27, 7.13 ± 6.16, 8.94 ± 5.11, 3.61 ± 3.33) and Kim-1 (14.60 ± 7.62, 19.28 ± 10.51, 13.49 ± 6.20, 8.70 ± 6.06) in the KIT-PR1P/VEGF group, PR1P/VEGF group, VEGF group and PBS group at I/R 24 h. ****P < 0.0001. All data are expressed as mean ± SD. (E) Fluorescence co-localisation analysis of Kim-1 and VEGF in the KIT-PR1P/VEGF group, PR1P/VEGF group, VEGF group and PBS group at I/R 6 h. (F) Fluorescence co-localisation analysis of Kim-1 and VEGF in the KIT-PR1P/VEGF group, PR1P/VEGF group, VEGF group and PBS group at I/R 24 h. (G)Quantitative ELISA assay for VEGF in kidney at 6 h and 24 h post-injection. At 6 h post-injection, KIT-PR1P/VEGF = 0.616 ± 0.077 μg/g, KIT-PR1P = 0.429 ± 0.057 μg/g, PR1P/VEGF = 0.406 ± 0.033 μg/g, VEGF = 0.449 ± 0.027 μg/g, PBS = 0.266 ± 0.019 μg/g. At 24 h post-injection, KIT-PR1P/VEGF = 0.378 ± 0.041 μg/g, KIT-PR1P = 0.278 ± 0.031 μg/g, PR1P/VEGF = 0.254 ± 0.041 μg/g, VEGF = 0.185 ± 0.025 μg/g, PBS = 0.162 ± 0.060 μg/g. Data are presented as mean ± SD. N = 4, ****P < 0.0001, ***P < 0.001, **P < 0.01, *P < 0.05. (H) Quantitative ELISA assay for VEGF in serum. At 6 h post-injection, KIT-PR1P/VEGF = 3.100 ± 2.453 pg/ml, KIT-PR1P = 5.978 ± 0.813 pg/ml, PR1P/VEGF = 12.783 ± 2.710 pg/ml,VEGF = 7.455 ± 2.315 pg/ml, PBS = 8.765 ± 0.885 pg/ml. At 24 h post-injection, KIT-PR1P/VEGF = 8.042 ± 2.113 pg/ml, KIT-PR1P = 16.243 ± 5.550 pg/ml, PR1P/VEGF = 10.776 ± 4.668 pg/ml,VEGF = 13.899 ± 4.964 pg/ml, PBS = 16.059 ± 4.776 pg/ml. Data are presented as mean ± SD. N = 4, *P < 0.05. (I) Western blot of VEGF in KIT-PR1P/VEGF group, KIT-PR1P group, PR1P/VEGF group, VEGF group and PBS group at I/R 6 h and 24 h after injection, and Statistical analysis of Western blot of VEGF in KIT-PR1P/VEGF, KIT-PR1P, PR1P/VEGF, VEGF and PBS at I/R 6 h and 24 h after injection. (Mean ± SD, N = 4, *P < 0.05, **P < 0.01, ***P < 0.001, ****P < 0.0001).

levels of CD31 expression in sections from the KIT-PR1P/VEGF group than from the PBS, VEGF and normal groups at 24 h, 72 h and 2w after injections respectively (Fig. 5A–C). Quantitative analysis of the mean fluorescence intensity level of CD31 in KIT-PR1P/VEGF group (117.729 ± 12.884 , 110.124 ± 16.672 , 111.536 ± 17.462) was increased compared to that of VEGF (92.993 ± 22.522 , 86.152 ± 13.585 , 82.473 ± 15.807) and PBS (78.679 ± 11.872 , 65.256 ± 6.957 , 74.677 ± 20.207) (Fig. 5D–F). These data suggested that due to the targeted delivery of VEGF in ischemic kidney, KIT-PR1P/VEGF could promote the angiogenesis and reconstruct the microcirculation which was lost during ischemic reperfusion injury.

3.6. KIT-PR1P/VEGF protected the kidney against renal I/R injury by inhibiting renal tubular epithelial cell apoptosis

VEGF was reported to protect kidney cells against hypoxic injury after renal ischemia [4].TUNEL staining was used to determine the number of apoptotic cells after renal I/R injury (Fig. 6A–F). The results showed that TUNEL-positive cells in the KIT-PR1P/VEGF group (2.54 ± 1.95 %, 2.42 ± 1.34 %, 6.04 ± 4.46 %) significantly decreased compared to those in the VEGF group (16.69 ± 9.54 %, 18.52 ± 4.90 %, 19.89 ± 11.76 %) and PBS group (40.65 ± 6.93 %, 29.57 ± 8.07 %, 41.37 ± 19.4 %) at 24 h, 72 h and 2w after intravenous injection. This finding revealed the potential protective effect of

A

Evaluation of renal function by Scr after I/R injury and intravenous administration

	24h,umol/L(N=6)	72h,umol/L(N=6)	2w,umol/L (N=6)
NORMAL	51.04±5.55****	51.41±6.17***	51.52±7.52***
KIT-PR1P/VEGF	134.76±60.08***	51.61±6.73***	56.13±6.58***
VEGF	192.62±75.01**	85.46±14.16	81.47±25.51
PBS	350.03±106.33	86.17±17.64	101.99±15.48

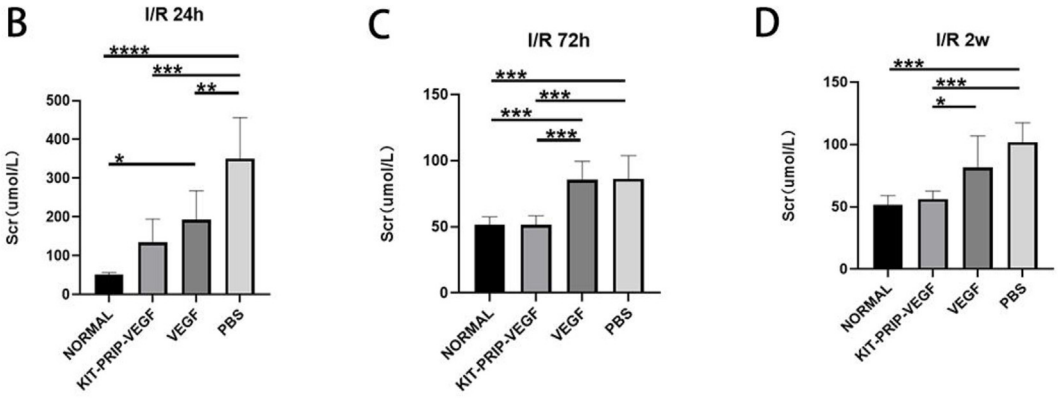

Fig. 3. The evaluation of renal function by serum Scr level after KIT-PR1P/VEGF intravenous injection. (A) Summary of Scr data for renal function after administration. ****P < 0.0001, ***P < 0.001. **P < 0.01. (B–D) Histogram of Scr assay for renal function after I/R injury and at 24 h, 72 h and 2w post-administration. All data are expressed as mean ± SD. ****P < 0.0001, ***P < 0.001, **P < 0.01, *P < 0.05. N = 6.

KIT-PR1P/VEGF against renal I/R injury. Caspase-3 was the most important terminal cleavage enzyme associated with apoptosis and was activated as cleaved Caspase-3 during the early stage of apoptosis [22,23]. Then immunofluorescence staining of cleaved Caspase-3 expression was performed at 24 h, 72 h and 2w post-administration. As shown in Fig. 6h-M, the mean fluorescent intensity of cleaved Caspase-3 in PBS group (731616 ± 439533 , 711531 ± 385039 , 2038637 ± 1385447) was significantly lower than that of KIT-PR1P/VEGF group (135583 ± 87900 , 105720 ± 40946 , 203379 ± 55394) and VEGF group (557117 ± 186282 , 436163 ± 183826 , 372152 ± 253363) but there was no statistical difference between KIT-PR1P/VEGF group and VEGF group at 24 h, 72 h and 2w after injection. These results revealed KIT-PR1P/VEGF could protect ischemic kidney and inhibit apoptosis of renal cells through decreasing the expression of pro-apoptotic proteins cleaved Caspase-3.

3.7. KIT-PR1P/VEGF protected the kidney from I/R injury by activating VEGF and its downstream cascade response

It was reported that VFGF protected against renal I/R injury by activating the AKT and ERK pathway [24,25]. Then the activation of VEGF downstream pathway was detected at 24 h after intravenous injection of KIT-PR1P/VEGF. As shown in Fig. 7 (A, B), immunofluorescence staining revealed the activation of p-VEGFR could be observed in KIT-PR1P/VEGF group (122.888 ± 9.915 , 114.492 ± 15.819 , 115.377 ± 18.364) compared with VEGF group (97.440 ± 15.470 , 91.612 ± 16.328 , 90.170 ± 12.223), PBS group (87.878 ± 13.766 , 56.170 ± 6.738 , 61.819 ± 14.095) and normal group (67.499 ± 4.071). And these results were further confirmed by Western blot in Fig. 7 (C, D). Consistent with the expression of p-VEGFR, the expression of p-AKT and p-ERK was also significantly increased in KIT-PR1P/VEGF group compared with KIT-PR1P, PR1P/VEGF, VEGF and PBS group (Fig. 7C, E-H). Therefore, these results demonstrated KIT-PR1P/VEGF could upregulate AKT and ERK signaling pathways for the recovery of renal ischemia.

4. Discussion

In response to special biological signals in regenerative environment, the construction of targeted growth factor delivery systems had become the focus in regenerative medicine and tissue engineering [5,6,26,27]. These targeted delivery systems could realize the spatiotemporal release in specific organs, increase the regional concentration, decrease the undesirable side effect of growth factor, and eventually promote tissue regeneration [28].

VEGF had been reported to benefit endothelial and epithelial cell proliferation. After tissue ischemic injury, VEGF could have a significant protective effect by promoting angiogenesis [29–31]. After renal ischemic injury, exogenous VEGF administration might be a viable approach to protect the kidney and improve hemodynamics [32]. In addition, VEGF was also involved in attenuating kidney fibrosis. For example, a series of extracellular vesicles derived from different stem cells was revealed to mediate renal injury and to prevent renal fibrosis by inducing the release of VEGF [4,33]. Other specific drugs such as sodium glucose cotransporter (SGLT) 2 inhibitor-luseogliflozin was shown to attenuate renal fibrosis also through VEGF dependent pathway after renal injury [34]. Currently, common approaches of VEGF delivery after AKI were non-targeted, and novel targeting delivery system of VEGF to injured renal tissue would facilitate the recovery of AKI [35].

The discovery of targeted peptides provided novel strategies for growth factor delivery. It had been reported that the specific peptide PR1P could specifically bind VEGF, and also promoted

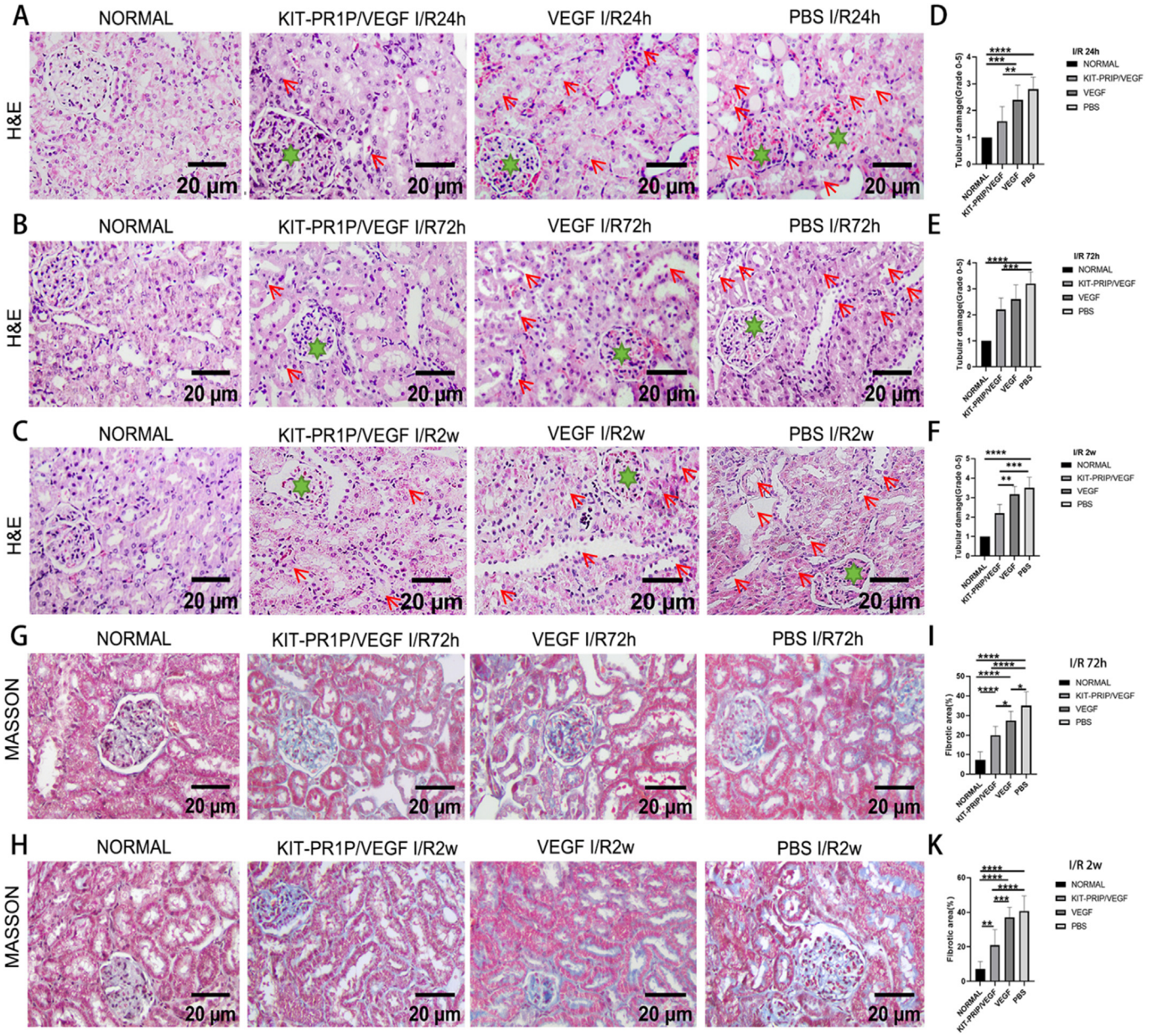

Fig. 4. Morphology evaluation of ischemic kidney after KIT-PR1P/VEGF intravenous injection. (A–C) Histopathological staining (H&E) for kidney pathological injury observation. Scale Bar = 20 μm. Red arrow indicated renal tubular injury; green asterisk indicated glomerulus. (D–F) Quantitative analysis of renal tubule injury based on H&E staining. (G–H) Masson staining of ischemic kidney after KIT-PR1P/VEGF intravenous injection. (I–K) Quantitative analysis of the area of renal interstitial fibrosis in obstructed kidneys. All data are expressed as mean ± SD. ****P < 0.0001, ***P < 0.001, **P < 0.01. N = 5.

angiogenesis by enhancing the formation of VEGF dimers [12,13]. In previous studies, PR1P was used to modify nano glass by chemical covalent coupling, which could immobilize VEGF and increase the bioactivity of scaffolds [13]. It also could connect with other specific peptide such as extracellular matrix (ECM) binding peptide (EBP peptide), that will specifically immobilize VEGF in ECM scaffolds [36]. The pro-angiogenic effect of VEGF, PR1P/VEGF, EBP-PR1P/VEGF was systematically compared, and the result showed both PR1P/VEGF and EBP-PR1P/VEGF could promote tube-formation *in vitro* compared with VEGF group but there was no difference between PR1P/VEGF and EBP-PR1P/VEGF group on pro-angiogenic effect. For kidney injury, Kim-1 immediately up-regulated after acute kidney injury, and specific peptide KIT was shown to guide growth factor to ischemic kidney in our previous studies [2]. We were interested whether bi-functional peptide KIT-PR1P could bind with VEGF and deliver VEGF to ischemic kidney. As a result, modified KIT-PR1P/VEGF was constructed and the targeting and therapeutic effect was explored in renal I/R model. Due to RP1P peptide didn't have targeting capacity and could not guide VEGF to ischemic kidney, so we didn't set PR1P/VEGF as control. As shown in Figs. 1 and 2, KIT-PR1P had stronger targeting ability for renal tubules than PR1P, and the ELISA assay also showed that due to the guidance of KIT-PR1P, significant more VEGF retained in ischemic kidney and less diffusion in blood than native VEGF. These results showed that KIT-PR1P/VEGF could specifically target ischemic kidney and reserve more VEGF in renal tissue after I/R ischemia. Then we evaluated the protective effect of KIT-PR1P/VEGF on ischemic kidney. The renal function of KIT-PR1P/VEGF group was significantly better than that of native VEGF group and PBS group at 24 h and 72 h after tail vein injection. Although the advantage of

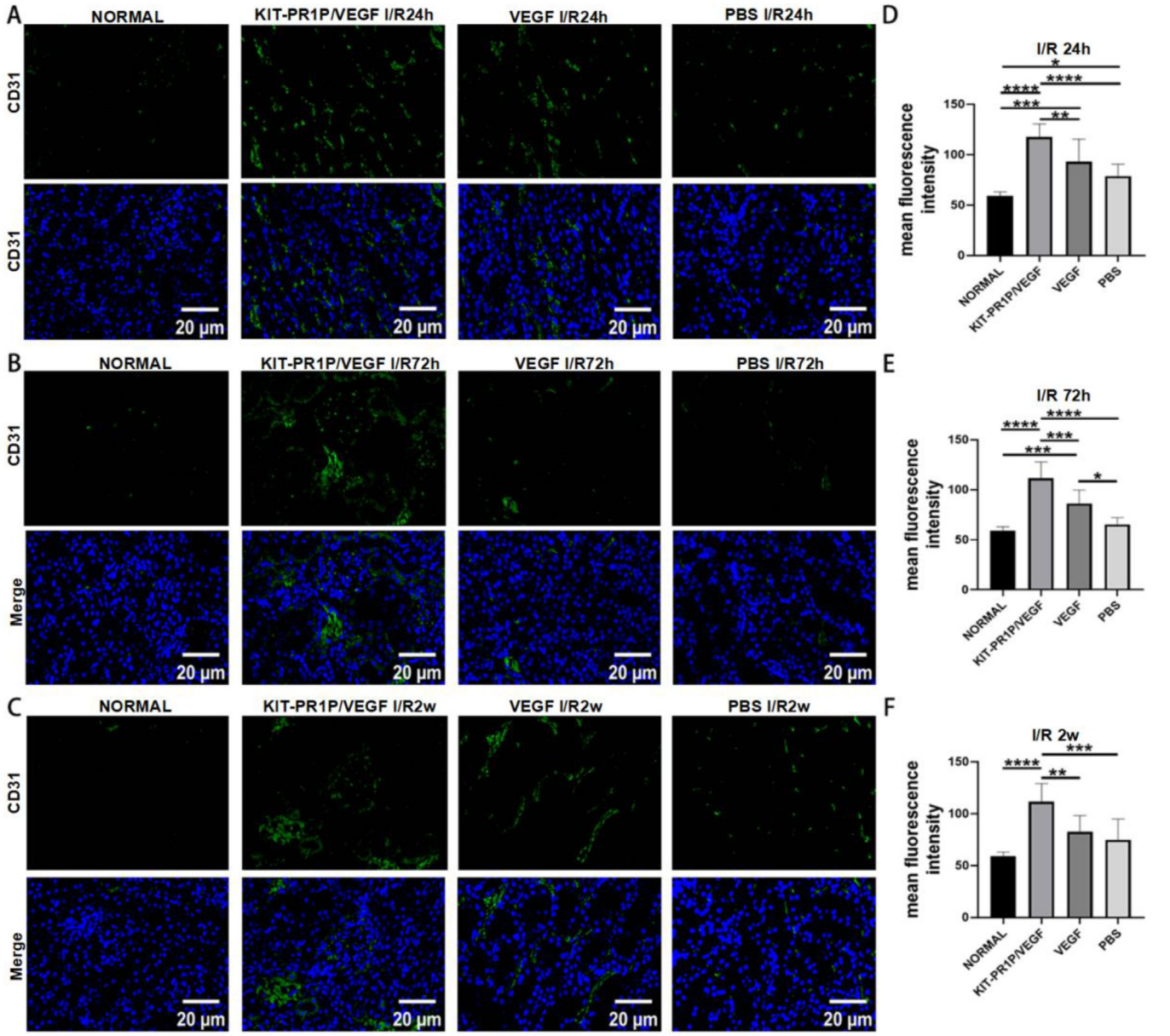

Fig. 5. Immunofluorescence staining of CD31 in ischemic kidney after KIT-PR1P/VEGF intravenous injection. Green fluorescence in this figure indicated areas stained positive for CD31, and blue fluorescence indicated DAPI. (A–C) Immunofluorescence staining for endothelial marker CD31 after I/R injury. Scale Bar = 20 μm. (D–F) Quantitative of Immunofluorescence staining for CD31. All data was expressed as mean ± SD.*P < 0.05, **P < 0.01, ***P < 0.001, ****P < 0.0001. N = 5.

KIT-PR1P/VEGF group over natural VEGF group was not obvious after 2w, the Scr level of KIT-PR1P/VEGF group was still greatly lower than that of PBS group within 2w after injection (Fig. 3). The results of pathological staining showed that compared with natural VEGF group and PBS group, KIT-PR1P/VEGF group significantly reduced renal tubular cell apoptosis, morphological damage and collagen fibrosis area (Figs. 4–6). These results were also consistent with the results of renal function assay, which showed that KIT-PR1P/VEGF could target the kidney injury site after I/R, deliver VEGF efficiently, and promote the functional recovery of ischemic kidney tissue.

Although Kim-1 was rarely expressed in normal mammalian kidneys, as a receptor that mediated apoptosis and oxidative lipid phagocytosis, its high expression after acute renal injury would directly promote renal inflammatory damage and fibrosis, which might be related to the up-regulation of pro-inflammatory cytokine monocyte chemoattractant protein-1 and the activation of rapamycin (mTOR) or MAPK pathway [7,37–39]. Apoptotic vesicles secreted by apoptotic renal tubular epithelial cells triggered the binding of Kim-1 to P85 protein, which stimulated the autophagic program and inhibited the activity of NF-κb, a transcription factor responsible for the production of pro-inflammatory cytokines [7,40]. Increased Kim-1 reduced levels of the inner cell receptor Nur77 which was an inducer of apoptosis and could prevent programmed cell death and enhance its survival ability under stressful environments [41]. Kim-1 had also been reported to promote the migration and proliferation of dedifferentiated cells in regenerating renal epithelial cells [42]. Van Timmeren et al. reported Kim-1 colocalized with Vimentin in proximal tubular cells and regulated them into dedifferentiated phenotype [43]. In present study, whether KIT-PR1P interacted with Kim-1 could participate the function of Kim-1 would be

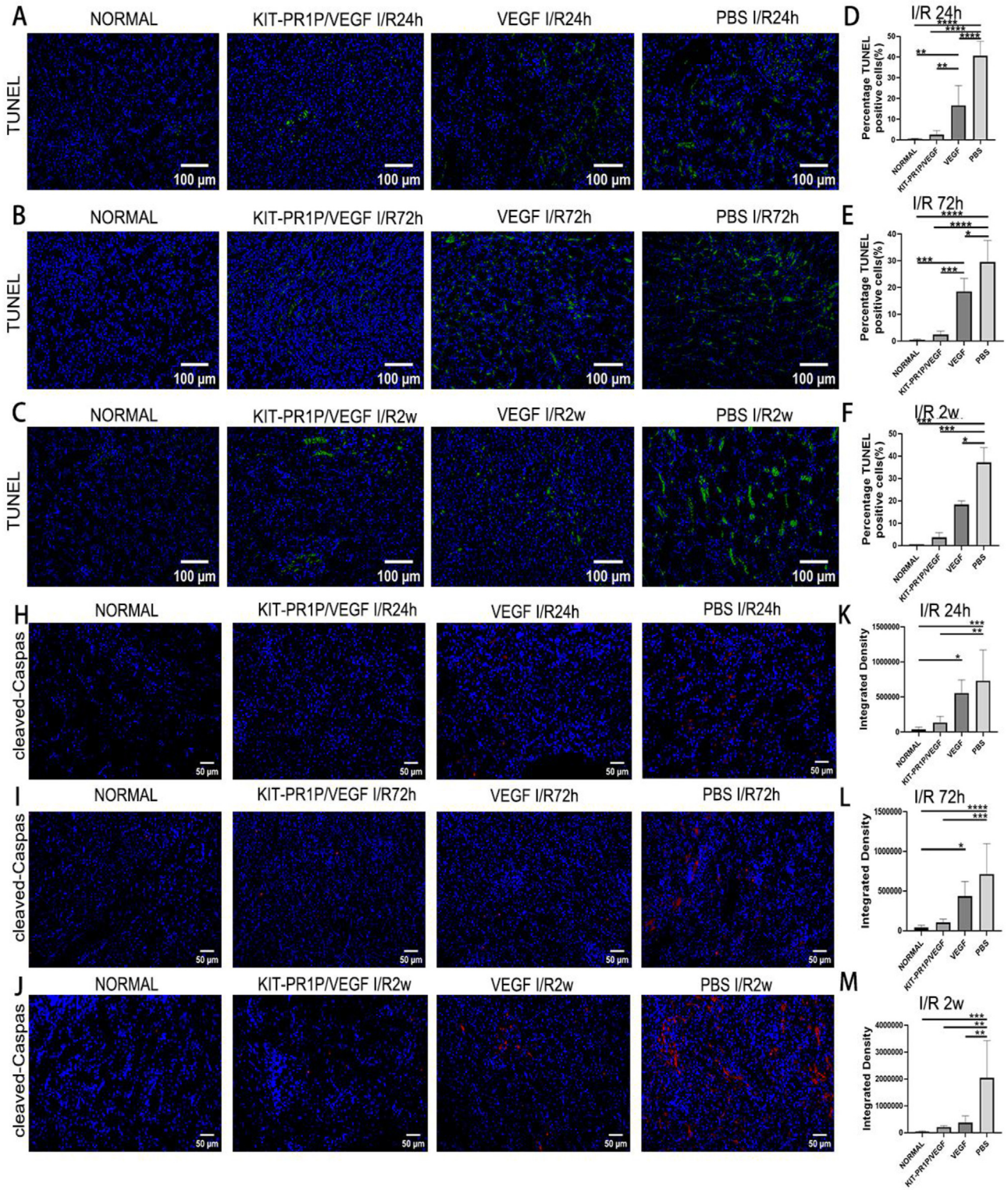

Fig. 6. TUNEL staining and Immunofluorescence staining of cleaved-Caspase3 in ischemic kidney after KIT-PR1P/VEGF intravenous injection. (A–C) TUNEL staining for apoptosis cells assessment (green). Scale Bar = 100 μm. (D–F) Quantitative of kidney TUNEL-positive cells. All data are expressed as mean ± SD. *P < 0.05, **P < 0.01, ***P < 0.001, ****P < 0.0001. N = 5. (H–J) Immunofluorescence staining of cleaved-Caspase3 in ischemic kidney after KIT-PR1P/VEGF intravenous injection. Red fluorescence indicated areas stained positive for cleaved-Caspase3, and blue fluorescence indicated DAPI. Immunofluorescence staining for cleaved-Caspase3 after I/R injury. Scale Bar = 50 μm. (K–M) Quantitative of Immunofluorescence staining for cleaved-Caspase3. All data was expressed as mean ± SD.*P < 0.05, **P < 0.01, ***P < 0.001, ****P < 0.0001. N = 5.

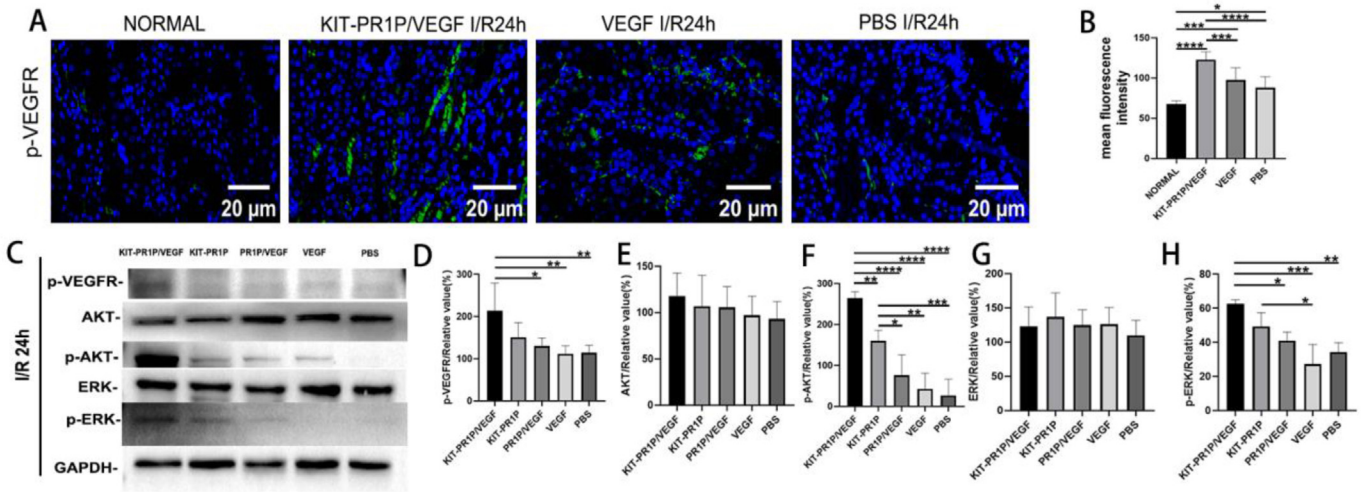

Fig. 7. Downstream pathway of KIT-PR1P/VEGF. (A) Immunofluorescence staining of p-VEGFR in ischemic kidney at 24 h intravenous injection of KIT-PR1P/VEGF after I/R injury and administration. Scale Bar = 20 μm. (B) Quantitative of IHF staining for p-VEGFR. All data are expressed as mean ± SD.*P < 0.05, ***P < 0.001, ****P < 0.0001. N = 5. (C) Western blotting assay of ischemia-reperfused kidneys for p-VEGFR, AKT, phospho-AKT, ERK, phospho-ERK at 24 h post administration. GAPDH was used as a control; (D) Statistical analysis of relative value for Western blot of p-VEGFR; (E) Statistical analysis of relative value for Western blot of AKT; (F) Statistical analysis of relative value for Western blot of p-AKT. (G) Statistical analysis of relative value for Western blot of ERK. (H) Statistical analysis of relative value for Western blot of p-ERK. N = 5. ****p < 0 0.0001, ***p < 0 0.001, **p < 0 0.01, *p < 0.05.

further detected. That might be one of the reasons that KIT-PR1P/VEGF decreased cell apoptosis, dedifferentiation and fibrosis. In addition, after KIT-PR1P/VEGF targeted binding to Kim-1, the large amounts of VEGF were retained and sustained released, then the downstream signalling pathway was detected. And KIT-PR1P/VEGF could activate phosphorylated VEGFR and further protect renal cells and reduce apoptosis after reperfusion injury through activation of AKT and ERK in the downstream cascade (Fig. 7). After ischemia-reperfusion injury, renal tubular epithelial cells underwent dedifferentiation, proliferation, migration and re-differentiation of the epithelial cell fraction after acute necrosis [44,45]. The protein mesenchymal initiation factor-Vimentin, a mesenchymal marker, was initially expressed only in renal mesenchymal cells and was involved in renal embryonic development [46]. In the setting of re-establishing blood oxygen supply after acute ischemia, Vimentin started to upregulate in dedifferentiated renal tubular epithelial cells and participated in the process of post-stress repair of renal tubular epithelial cells [47–50]. We found by immunohistochemical staining that KIT-PR1P/VEGF significantly blocked the expression of Vimentin after I/R injury in rats, indicating the targeting release of VEGF could prevent the mesenchymal transformation and protect kidney in the early stage of renal injury (Supplementary Fig. 3).

We also explored the protective effect of KIT-PR1P/VEGF on kidney cells after injury by TUNEL assay, with a significant reduction in the number of positive apoptotic cells. And we further validated that KIT-PR1P/VEGF inhibited apoptosis after renal ischemia-reperfusion injury by detecting cleaved caspase-3, a marker of apoptosis (Fig. 6). Zhang, B. et al. revealed that apoptosis were key events of the occurrence and development of I/R injury at the molecular level. Recent studies had shown that mitochondrial dysfunction was also key factor leading to oxidative stress and apoptosis in renal ischemia reperfusion (I/R) disease. They found that hypoxia/reoxygenation led to increased mitochondrial division and decreased mitochondrial fusion in human renal tubular epithelial cells (HK-2) [51]. Whether KIT-PR1P/VEGF would impact mitochondrial function and apoptosis needed to further explore.

5. Conclusion

To sum up, we had designed and constructed a safe and efficient bi-functional KIT-PR1P peptide, which could recognize and target the Kim-1 signal released from the early renal injury after I/R, then deliver and retain active VEGF *in vitro* and *in vivo*. When it combined with VEGF for the treatment of AKI by tail vein injection in rat model, the KIT-PR1P/VEGF increased angiogenesis, decreased cell apoptosis, tubular injury, and attenuated fibrosis and mesenchymal transformation of epithelial cells, finally promoted the recovery of renal function. Additionally, the AKT/ERK pathways involved in the process of KIT-PR1P/VEGF for the repair of renal I/R. It provided a potential strategy for the targeting delivery of VEGF in the therapy of AKI.

Funding

This study was supported by National Natural Science Foundation of China under Grant (81970590), Natural Science Foundation of Shandong Province under Grant (ZR2023MC168) and Chongqing Science and Technology Commission under Grant (CSTB2022NSCQ-MSX0157).

Data availability statement

All data required of the paper are included in the paper.

Declaration of competing interest

The author(s) declared no potential conflicts of interest with respect to the research, authorship, and/or publication of this article.

Acknowledgements

Not applicable.

Appendix A. Supplementary data

Supplementary data to this article can be found online at https://doi.org/10.1016/j.reth.2023.12.014.

References

[1] Bellomo R, Kellum JA, Ronco C. Acute kidney injury. Lancet 2012;380(9843):756–66.
[2] Song S, Hou X, Zhang W, Liu X, Wang W, Wang X, et al. Specific bFGF targeting of Kim-1 in ischemic kidneys protects against renal ischemia-reperfusion injury in rats. Regen Biomater 2022;9:rbac029.
[3] Nankivell BJ, Borrows RJ, Fung CL, O'Connell PJ, Allen RD, Chapman JR. The natural history of chronic allograft nephropathy. N Engl J Med 2003 Dec 11;349(24):2326–33.
[4] Zhong X, Tang TT, Shen AR, Cao JY, Jing J, Wang C, et al. Tubular epithelial cells-derived small extracellular vesicle-VEGF-A promotes peritubular capillary repair in ischemic kidney injury. NPJ Regen Med 2022 Dec 17;7(1):73.
[5] Lu Y, Aimetti AA, Langer R, Gu Z. Bioresponsive materials. Nat Rev Mater 2016;1:16075.
[6] Mi P, Cabral H, Kataoka K. Ligand-installed nanocarriers toward precision therapy. Adv Mater 2020 Apr;32(13):e1902604.
[7] Yang L, Brooks CR, Xiao S, Sabbisetti V, Yeung MY, Hsiao LL, et al. Kim-1-mediated phagocytosis reduces acute injury to the kidney. J Clin Invest 2015 Apr;125(4):1620–36.
[8] Bland SK, Schmiedt CW, Clark ME, DeLay J, Bienzle D, et al. Expression of kidney injury molecule-1 in healthy and diseased feline kidney tissue. Vet Pathol 2017 May;54(3):490–510.
[9] Bonventre JV, Yang L. Kidney injury molecule-1. Curr Opin Crit Care 2010 Dec;16(6):556–61.
[10] Tang TT, Wang B, Li ZL, Wen Y, Feng ST, Wu M, et al. Kim-1 targeted extracellular vesicles: a new therapeutic platform for RNAi to treat AKI. J Am Soc Nephrol 2021 Oct;32(10):2467–83.
[11] Haque ME, Khan F, Chi L, Gurung S, Vadevoo SMP, Park RW, et al. A phage display-identified peptide selectively binds to kidney injury molecule-1 (Kim-1) and detects kim-1-overexpressing tumors in vivo. Cancer Res Treat 2019 Jul;51(3):861–75.
[12] Adini A, Adini I, Chi ZL, Derda R, Birsner AE, Matthews BD, et al. A novel strategy to enhance angiogenesis in vivo using the small VEGF-binding peptide PR1P. Angiogenesis 2017 Aug;20(3):399–408.
[13] Schumacher M, Habibovic P, van Rijt S. Peptide-modified nano-bioactive glass for targeted immobilization of native VEGF. ACS Appl Mater Interfaces 2022 Feb 2;14(4):4959–68.
[14] Mohseni N, Jahanian-Najafabadi A, Kazemi-Lomedasht F, Arezomand R, Habibi-Anbouhi M, Shahbazzadeh D, et al. Recombinant expression and purification of functional vascular endothelial growth factor-121 in the baculovirus expression system. Asian Pac J Tropical Med 2016 Dec;9(12):1195–9.
[15] Wang S, Umrath F, Cen W, Reinert S, Alexander D. Angiogenic potential of VEGF mimetic peptides for the biofunctionalization of collagen/hydroxyapatite composites. Biomolecules 2021 Oct 19;10:11.
[16] Specific bFGF targeting of Kim-1 in ischemic kidneys protects against renal ischemia reperfusion injury in rats.
[17] Villanueva S, Cespedes C, Gonzalez AA, Roessler E, Vio CP. Inhibition of bFGF-receptor type 2 increases kidney damage and suppresses nephrogenic protein expression after ischemic acute renal failure. Am J Physiol Regul Integr Comp Physiol 2008 Mar;294(3):R819–28.
[18] Villanueva S, Contreras F, Tapia A, Carreno JE, Vergara C, Ewertz E, et al. Basic fibroblast growth factor reduces functional and structural damage in chronic kidney disease. Am J Physiol Ren Physiol 2014;306(4):F430–41.
[19] Moore MA, Hattori K, Heissig B, Shieh JH, Dias S, Crystal RG, et al. Mobilization of endothelial and hematopoietic stem and progenitor cells by adenovector-mediated elevation of serum levels of SDF-1, VEGF, and angiopoietin-1. Ann N Y Acad Sci 2001 Jun;938:36–45. discussion 45-7.
[20] Zisa D, Shabbir A, Mastri M, Suzuki G, Lee T. Intramuscular VEGF repairs the failing heart: role of host-derived growth factors and mobilization of progenitor cells. Am J Physiol Regul Integr Comp Physiol 2009 Nov;297(5):R1503–15.
[21] Chade AR. VEGF: potential therapy for renal regeneration. F1000 Med Rep 2012;4:1.
[22] Fernandes-Alnemri T, Litwack G, Alnemri ES. CPP32, a novel human apoptotic protein with homology to Caenorhabditis elegans cell death protein Ced-3 and mammalian interleukin-1 beta-converting enzyme. J Biol Chem 1994 Dec 9;269(49):30761–4.
[23] Fernandes-Alnemri T, Takahashi A, Armstrong R, Krebs J, Fritz L, Tomaselli K, et al. Mch3, a novel human apoptotic cysteine protease highly related to CPP32. Cancer Res 1995 Dec 15;55(24):6045–52.
[24] Tan H, Chen J, Li Y, Zhong Y, Li G, Liu L. Glabridin, a bioactive component of licorice, ameliorates diabetic nephropathy by regulating ferroptosis and the VEGF/Akt/ERK pathways. Mol Med 2022 May 20;28(1):58.
[25] Wang X, Jiang L, Liu XQ, Huang YB, Wang AL, Zeng HX, et al. Paeoniflorin binds to VEGFR2 to restore autophagy and inhibit apoptosis for podocyte protection in diabetic kidney disease through PI3K-AKT signaling pathway. Phytomedicine 2022 Nov;106:154400.
[26] Anderson MA, O'Shea TM, Burda JE, Ao Y, Barlatey SL, Bernstein AM, et al. Required growth facilitators propel axon regeneration across complete spinal cord injury. Nature 2018 Sep;561(7723):396–400.
[27] Gulfam M, Sahle FF, Lowe TL. Design strategies for chemical-stimuli-responsive programmable nanotherapeutics. Drug Discov Today 2019 Jan;24(1):129–47.
[28] Shi C, Zhao Y, Yang Y, Chen C, Hou X, Shao J, et al. Collagen-binding VEGF targeting the cardiac extracellular matrix promotes recovery in porcine chronic myocardial infarction. Biomater Sci 2018 Jan 30;6(2):356–63.
[29] Acarregui MJ, Ramirez K, Brown KR, Mallampalli RK. Vascular endothelial growth factor (VEGF) induces airway epithelial cell proliferation and surfactant protein gene expression in human fetal lung in vitro † 242. Pediatr Res 1998;43(4):44.
[30] Zhao H, Huang H, Alam A, Chen Q, Suen KC, Cui J, et al. VEGF mitigates histone-induced pyroptosis in the remote liver injury associated with renal allograft ischemia-reperfusion injury in rats. Am J Transplant 2018 Aug;18(8):1890–903.
[31] Kundu N, Nandula SR, Asico LD, Fakhri M, Banerjee J, Jose PA, et al. Transplantation of apoptosis-resistant endothelial progenitor cells improves renal function in diabetic kidney disease. J Am Heart Assoc 2021 Apr 6;10(7):e019365.
[32] Eirin A, Lerman LO. Stem cell-derived extracellular vesicles for renal repair: do cardiovascular comorbidities matter? Am J Physiol Ren Physiol 2019 Dec 1;317(6):F1414–9.
[33] Medica D, Franzin R, Stasi A, Castellano G, Migliori M, Panichi V, et al. Extracellular vesicles derived from endothelial progenitor cells protect human glomerular endothelial cells and podocytes from complement- and cytokine-mediated injury. Cells 2021 Jul 2;10(7).
[34] Zhang Y, Nakano D, Guan Y, Hitomi H, Uemura A, Masaki T, et al. A sodium-glucose cotransporter 2 inhibitor attenuates renal capillary injury and fibrosis by a vascular endothelial growth factor-dependent pathway after renal injury in mice. Kidney Int 2018 Sep;94(3):524–35.
[35] Guise E, Chade AR. VEGF therapy for the kidney: emerging strategies. Am J Physiol Ren Physiol 2018 Oct 1;315(4):F747–51.
[36] Cao W, Zhang H, Zhou N, Zhou R, Zhang X, Yin J, et al. Functional recovery of myocardial infarction by specific EBP-PR1P peptides bridging injectable cardiac extracellular matrix and vascular endothelial growth factor. J Biomed Mater Res 2022 Dec 29;111(7):1549–3296.
[37] Yin W, Naini SM, Chen Hentschel DM, Humphreys BD, Bonventre JV G. Mammalian target of rapamycin mediates kidney injury molecule 1-dependent tubule injury in a surrogate model. J Am Soc Nephrol 2016 Jul;27(7):1943–57.
[38] Kirk R. Renal fibrosis: Kim-1 expression links kidney injury with CKD in mice. Nat Rev Nephrol 2013 Nov;9(11):627.
[39] Humphreys BD, Xu F, Sabbisetti V, Grgic I, Movahedi Naini S, Wang N, et al. Chronic epithelial kidney injury molecule-1 expression causes murine kidney fibrosis. J Clin Invest 2013 Sep;123(9):4023–35.
[40] Brooks CR, Yeung MY, Brooks YS, Chen H, Ichimura T, Henderson JM, et al. Kim-1-/TIM-1-mediated phagocytosis links ATG5-/ULK1-dependent clearance of apoptotic cells to antigen presentation. EMBO J 2015 Oct 1;34(19):2441–64.
[41] Balasubramanian S, Jansen M, Valerius MT, Humphreys BD, Strom TB. Orphan nuclear receptor Nur77 promotes acute kidney injury and renal epithelial apoptosis. J Am Soc Nephrol 2012;23(4):674–86.
[42] Zhang Z, Cai CX. Kidney injury molecule-1 (Kim-1) mediates renal epithelial cell repair via ERK MAPK signaling pathway. Mol Cell Biochem 2016 May;416(1–2):109–16.
[43] van Timmeren MM, van den Heuvel MC, Bailly V, Bakker SJ, van Goor H, Stegeman CA. Tubular kidney injury molecule-1 (Kim-1) in human renal disease. J Pathol 2007 Jun;212(2):209–17.
[44] Kumar S. Cellular and molecular pathways of renal repair after acute kidney injury. Kidney Int 2018 Jan;93(1):27–40.
[45] Rayego-Mateos S, Marquez-Exposito L, Rodrigues-Diez R, Sanz AB, Guiteras R, Dolade N, et al. Molecular mechanisms of kidney injury and repair. Int J Mol Sci 2022 Jan 28;3:23.
[46] Veller-Fornasa C, Gallina P. Recurrent aphthous stomatitis as an expression of pathergy in atopics. Acta Dermatovenerol Alpina Pannonica Adriatica 2006 Sep;15(3):144–7.
[47] Witzgall R, Brown D, Schwarz Bonventre JV C,. Localization of proliferating cell nuclear antigen, vimentin, c-Fos, and clusterin in the postischemic kidney. Evidence for a heterogenous genetic response among nephron segments, and a large pool of mitotically active and dedifferentiated cells. J Clin Invest 1994 May;93(5):2175–88.
[48] Villanueva S, Cespedes C, Vio CP. Ischemic acute renal failure induces the expression of a wide range of nephrogenic proteins. Am J Physiol Regul Integr Comp Physiol 2006 Apr;290(4):R861–70.
[49] Little MH, Kairath P. Does renal repair recapitulate kidney development? J Am Soc Nephrol 2017 Jan;28(1):34–46.
[50] Pasten C, Lozano M, Mendez GP, Irarrazabal CE. 1400W prevents renal injury in the renal cortex but not in the medulla in a murine model of ischemia and reperfusion injury. Cell Physiol Biochem 2022 Oct 19;56(5):573–86.
[51] Mao H, Zhang Y, Xiong Y, Zhu Z, Wang L, Liu X. Mitochondria-targeted antioxidant mitoquinone maintains mitochondrial homeostasis through the sirt3-dependent pathway to mitigate oxidative damage caused by renal ischemia/reperfusion. Oxid Med Cell Longev 2022;2022:2213503.